A NANOMATERIAL-BASED BIOSENSOR FOR THE QUANTITATIVE DETECTION OF ENROFLOXACIN RESIDUES IN RAW CHICKEN

Y. Shen, Y. He, Y. Fu, J. Wang, J. Zhang, M. Liao, Y. Li

HIGHLIGHTS

- A nanobiosensor was developed for rapid detection of enrofloxacin residues in chicken meat.
- 5-Sulfosalicylic acid was adopted in a facile method for pretreatment of chicken meat samples.
- The detection limit of 14.1 μg kg^{-1} was below the maximum residue limit for chicken meat.
- The total detection time from sample pretreatment to result report was less than 1.5 h.

ABSTRACT. *Antibiotic residues in animal-derived food products have been identified as a potential hazard in human health. Hence, a rapid, simple, and cost-effective method for detection of antibiotics in the food supply chain is highly desirable. The objective of this study was to develop a nanomaterial-based biosensor using immunomagnetic beads (IMBs) and quantum dots (QDs) for rapid and sensitive detection of enrofloxacin (ENR) residues in raw chicken. A 5-sulfosalicylic acid-based pretreatment method was adopted to extract ENR from chicken meat and reduce non-specific adsorption caused by complex food matrices. Two sensing elements were designed and fabricated: antibody functionalized IMBs and ENR-bovine serum albumin (BSA) conjugates modified QDs (QDs-BSA-ENR). Target ENR in samples was first captured and separated by IMBs, and then QDs-BSA-ENR, serving as a competitor and detection probe, was used to react with the residual binding sites on the IMB surfaces. With the presence of captured ENR, the binding of QDs-BSA-ENR to IMBs was competitively inhibited. Finally, the fluorescence intensity of reporting QDs in the QDs-BSA-ENR-IMBs complex at a wavelength of 614 nm was measured for the quantitation of target antibiotics. Under the optimum conditions, the proposed method allowed sensitive detection of ENR in a linear range from 1 to 100 ng mL^{-1} with a limit of detection (LOD) of 0.94 ng mL^{-1}. The LOD for spiked chicken meat was 14.1 μg kg^{-1}, which was below the maximum residue limits (MRLs) regulated in China and the European Union. The whole analytical procedure from food sampling to result report could be finished in less than 1.5 h. This nanobiosensor showed high potential for rapid and low-cost detection of ENR residues in the poultry supply chain to enhance food safety.*

Keywords. *Enrofloxacin, Immunomagnetic beads, Nanobiosensor, Poultry, Quantum dots, Rapid detection.*

Enrofloxacin (ENR), belonging to the family of fluoroquinolones, is a kind of synthetic antibiotic with broad-spectrum antimicrobial activity against most Gram-negative and some Gram-positive bacteria (Bonassa et al., 2017; Ellerbrock et al., 2019; Paudel et al., 2019; Sultan, 2014). ENR has been intensively used for treating bacterial infections and promoting animal growth in poultry and livestock (Huang et al., 2013; Rezende et al., 2019). However, ENR can accumulate in the human body through the food chain, which may pose a serious risk to human health via two main ways: adverse drug reactions and potential prevalence of antibiotic-resistant bacteria and genes (Pan et al., 2018). ENR can damage the digestive system, nervous system, liver, and kidneys and cause allergic reactions and imbalance of intestinal microflora (Sultan, 2014; Wang et al., 2017). Moreover, long-term exposure to the antibiotics can make pathogens become more resistant, which leads to ineffectiveness of antibacterial therapies (Terrado-Campos et al., 2017; Yasini et al., 2015). Given its potential hazards, some countries and organizations have set maximum residue limits (MRLs) for ENR in different animal-derived food products. For example, the MRLs for the sum of ENR and its major metabolite ciprofloxacin in animal muscle is 100 μg kg^{-1}, as regulated by both China and the European Union (Huang et al., 2013).

Submitted for review on 9 January 2020 as manuscript number PRS 13874; approved for publication as a Research Article by the Processing Systems Community of ASABE on 6 August 2020.

The authors are **Yafang Shen,** Graduate Student, College of Biosystems Engineering and Food Science, Zhejiang University, Hangzhou, China, and Department of Biological and Agricultural Engineering, University of Arkansas, Fayetteville, Arkansas; **Yawen He,** Graduate Student, **Yingchun Fu,** Professor, and **Jianping Wang,** Professor, College of Biosystems Engineering and Food Science, Zhejiang University, Hangzhou, China; **Jianmin Zhang,** Associate Professor, and **Ming Liao,** Professor, College of Veterinary Medicine, South China Agricultural University, Guangzhou, China; **Yanbin Li,** Distinguished Professor, Department of Biological and Agricultural Engineering, University of Arkansas, Fayetteville, Arkansas. **Corresponding author:** Yanbin Li, 203 Engineering Hall, University of Arkansas, Fayetteville, AR 72701; phone: 479-575-2881; e-mail: yanbinli@uark.edu.

Vol. 63(6): 1869-1878 ISSN 2151-0032 https://doi.org/10.13031/trans.13874

Numerous methods have been developed for ENR detection to implement legislative regulations and promote food safety. Chromatographic methods, including high-performance liquid chromatography (HPLC) and liquid chromatography-mass spectrometry (LC-MS), are still the most conventional and recommended methods for ENR detection (Huang et al., 2018; Junza et al., 2016; Yang et al., 2020). They possess high sensitivity and accuracy but also exhibit some inherent drawbacks, such as the requirement for expensive equipment and well-trained personnel, which restrict their applications to the laboratory scale. Rapid detection methods, such as enzyme-linked immunosorbent assay (ELISA) and lateral flow assays (Hu et al., 2019; Li et al., 2019), have been well developed for facile and rapid screening propose, but they show deficiencies in sensitivity and accuracy. Compared to these methods, biosensors appear to be alternative tools for antibiotic detection due to their advantages of rapid detection, high sensitivity, and potential for in-field application. Novel biosensing strategies, including graphene oxide and aptamer-based Förster resonance energy transfer biosensors (Dolati et al., 2018), upconversion nanoparticle-based luminescent biosensors (Liu et al., 2016, 2017), covalent organic framework-based electrochemical aptasensors (Wang et al., 2019), and surface plasmon resonance immunosensors (Pan et al., 2017), have been reported to detect ENR at extremely low limits of detection (LODs), even reaching fg mL^{-1}. However, their applications, especially in complex food matrices, should be further improved. Therefore, the development of a rapid, facile, and sensitive biosensor that performs well for ENR detection in actual food samples is highly desirable.

Immunomagnetic beads (IMBs), with recognition molecules (e.g., antibodies) coated on their surfaces, are usually considered a suitable tool to capture, concentrate, and separate target analytes from complex food matrices prior to detection. IMBs have received significant attention due to their large surface area, fast reaction kinetics, quick response to magnetic fields, and biocompatibility with biomolecules (Ji et al., 2016; Kim and Searson, 2015; Moro et al., 2017). Furthermore, they can be easily integrated into a transducer to improve detection sensitivity and specificity. Semiconductor quantum dots (QDs), displaying unique optical properties, are attracting great attention as novel fluorescent transducers. QDs have several advantages over conventional fluorophores, such as broad excitation spectra; narrow, size-tunable, and symmetric emission; improved brightness; long fluorescence lifetime; and good photostability (Chen et al., 2019; Goryacheva et al., 2019; Wegner and Hildebrandt, 2015).

Biosensing strategies based on magnetic separation and QD labeling have been reported for the detection of some small molecules, such as cancer TF-antigen and microcystin-LR, in a competitive format (Li et al., 2013; Yu et al., 2011). However, to the best of our knowledge, no published reports have focused on facile and rapid detection of ENR in poultry products.

In this study, a nanomaterial-based biosensor using IMBs and QDs as sensing elements was developed for sensitive detection of ENR in raw chicken (fig. 1). Prior to detection, a 5-sulfosalicylic acid-based pretreatment method was adopted to extract ENR from chicken meat and reduce non-specific adsorption caused by complex food matrices. Target ENR residues in samples were first captured and separated by IMBs, where they occupied the binding sites on the IMB surfaces. Second, ENR-bovine serum albumin (BSA) conjugates modified QDs (QDs-BSA-ENR), serving as a competitor and fluorescent label, could specifically bind to the IMBs via immunoreaction but was competitively inhibited in the presence of the target ENR, which in turn led to a decrease in the fluorescence signals. Finally, the fluorescence signals of the separated QDs-BSA-ENR-IMBs complexes were measured for ENR quantitation. The results showed that this nanobiosensor provided rapid and sensitive detection of ENR in both buffer and chicken meat samples and has potential for rapid detection of ENR in the poultry supply chain.

Materials and Methods

Materials and Apparatus

Carboxyl CdSe/ZnS core/shell QDs (QDs-COOH) with a maximum emission wavelength of 614 nm (8 μM) and carboxyl magnetic beads (MBs-COOH) with a diameter of 150 nm (10 mg mL^{-1}) were obtained from Ocean NanoTech (San Diego, Cal.). Monoclonal antibody against ENR (1 mg mL^{-1})

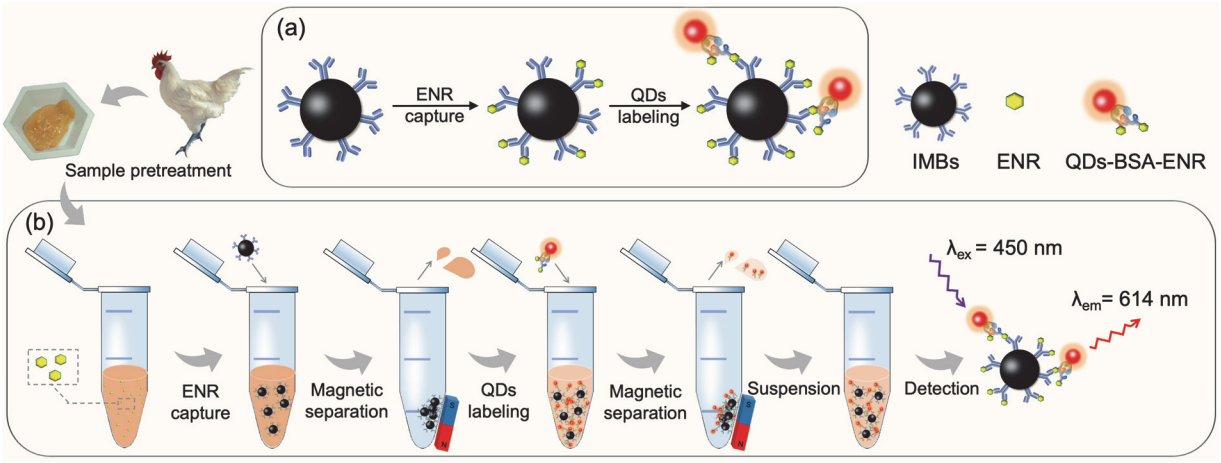

Figure 1. Illustration of proposed biosensing method for rapid detection of ENR residues in raw chicken: (a) principle and (b) procedure.

was purchased from Cusabio Biotech (Wuhan, China). Ciprofloxacin hydrochloride (CIP), ENR, 5-sulfosalicylic acid, and N-hydroxysulfosuccinimide sodium salt (Sulfo-NHS) were purchased from Aladdin Chemistry (Shanghai, China). N-(3-(dimethylaminopropyl)-N′-ethylcarbodiimide hydrochloride (EDC) was purchased from Sigma-Aldrich (St. Louis, Mo.). Oxytetracycline hydrochloride (OTC), chloramphenicol (CAP), kanamycin sulfate (KAN), doxycycline hydrochloride (DOX), tetracycline hydrochloride (TET), and BSA were obtained from Sangon Biotech (Shanghai, China). Levofloxacin (LEV) and norfloxacin (NOR) were purchased from Macklin Biochemical (Shanghai, China). All of the other chemicals were analytical grade or better quality and used without any further purification. Raw chicken breast was bought from a local supermarket. Deionized water (18.2 MΩ·cm) processed with a Milli-Q system (Millipore, Bedford, Mass.) was used throughout the experiment.

The fluorescence measurement was carried out using a Synergy H1 Hybrid Multi-Mode Microplate Reader (BioTek Instruments, Winooski, Vt.) equipped with Gen5 2.0 Data Analysis Software. The UV-vis spectra were obtained on a UV-vis spectrophotometer (8453, Agilent Technologies, Santa Clara, Cal.). A Nicolet Avatar 370 spectrometer (Thermo, Waltham, Mass.) was used to collect Fourier transform infrared (FTIR) spectra. The zeta potential of nanoparticles was determined using a Zetasizer Nano ZS-90 (Malvern Instruments, Malvern, U.K.).

Synthesis of BSA-ENR Conjugates

BSA-ENR conjugates were synthesized through the formation of amide bonds between the amino groups in BSA and the carboxyl groups in ENR in the presence of EDC and Sulfo-NHS, based on a previously reported method with some modifications (Poller et al., 2015). In brief, 20 mg of ENR, 10 mg of Sulfo-NHS, and 12.5 mg of EDC were suspended in 1 mL of dimethylformamide (DMF), and the mixture was gently stirred in the dark overnight for activation of the carboxyl groups in ENR. Afterward, the activated ENR solution was added dropwise into 3 mL of 10 mM phosphate buffered saline (PBS, pH 7.4) containing 50 mg of BSA and stirred for 3 h in the dark. The reaction solution was then dialyzed against 10 mM PBS for 3 days at 4°C, followed by centrifugation at 3,000 rpm for 5 min. The supernatant was collected, diluted to 1 mg mL^{-1} (calculated as the concentration of BSA), and stored at 4°C.

Preparation of QDs-BSA-ENR Probes

QDs-BSA-ENR probes were prepared according to a classic carbodiimide method with some modifications (Lisi et al., 2012). First, 10 μL of QDs-COOH was suspended in 200 μL of EDC and Sulfo-NHS solution (10 mM EDC and 15 mM Sulfo-NHS dissolved in 25 mM of 2-(N-morpholino)ethanesulfonic acid buffer (MES, pH 6.0)) and gently shaken in the dark. After 40 min of activation, the mixture was transferred into a centrifugal ultrafiltration unit (50 kDa MWCO), where it was centrifuged at 12,000 rpm for 5 min to remove excess EDC, Sulfo-NHS, and byproducts. The purified activated QDs were then resuspended in 160 μL of 10 mM boric acid-borax buffer (BB, pH 7.4), followed by the addition of 40 μL of BSA-ENR conjugates. The mixture reacted in the dark for 2.5 h with continuous stirring, and then 200 μL of BSA solution with a concentration of 2% was added, and the mixture was shaken for 1 h to block the unreacted sites on the QD surfaces. The free BSA-ENR conjugates and byproducts were removed by three cycles of ultrafiltration (100 kDa MWCO). Finally, the synthesized QDs-BSA-ENR probes were resuspended in 400 μL of 10 mM PBS buffer (pH 7.4) and stored at 4°C for further use.

Fabrication of IMBs

To prepare the IMBs (Liu et al., 2015; Yang et al., 2016), 10 μL of MBs-COOH, washed three times with 25 mM MES buffer containing 0.01% Tween-20, was suspended in 400 μL of freshly made EDC (10 mM) and Sulfo-NHS (15 mM) solution and gently stirred for 30 min. The excess EDC, Sulfo-NHS, and byproducts were then removed by magnetic separation using a magnetic scaffold, and the activated MBs-COOH were resuspended in 400 μL of 10 mM BB buffer containing 0.01% Tween-20. Simultaneously, 4 μL of monoclonal antibody against ENR was added to the activated MBs-COOH solution, and the mixture was stirred for 2.5 h at room temperature. Afterward, the unreacted sites on the IMB surfaces were blocked by 1% BSA for 1 h. The IMB conjugates were separated from free antibodies after three cycles of washing, resuspended in 100 μL of 10 mM PBS buffer (pH 7.4) containing 0.01% Tween-20 (PBST), and stored at 4°C for further use.

Competitive Fluorescence Assay for ENR Detection

In a typical experiment, 180 μL of ENR solution with different concentrations (10^{-2} to 10^{5} ng mL^{-1}) was mixed with 20 μL of IMBs and gently shaken at room temperature for 10 min. Free IMBs and ENR-IMBs composites were then isolated from the mixture by magnetic separation using a magnetic scaffold and then resuspended in 196 μL of 10 mM PBS buffer (pH 6.0) containing 0.1% BSA and 0.05% Tween-20. Afterward, 4 μL of QDs-BSA-ENR probes were added to the solution, and the mixture was allowed to react at room temperature for 30 min to form QDs-BSA-ENR-IMBs complexes. After magnetic separation and washing with 200 μL of PBST buffer, the fluorescence intensity of the QDs on the IMB surfaces was measured using a microplate reader with excitation at 450 nm. Before each addition of QDs-BSA-ENR probes and fluorescence detection, the IMBs, which had bonded with ENR in a sample and/or in the probes, were magnetically separated and washed three times with PBST buffer.

Preparation of Spiked Chicken Samples

A 5-sulfosalicylic acid-based pretreatment method was adopted, referring to Cui et al. (2015) with some modifications, to extract ENR from chicken meat and reduce nonspecific adsorption caused by complex food matrices. In brief, chicken meat was minced and homogenized; 1 g of tissue homogenate was spiked with different concentrations of ENR and incubated at room temperature for 2 h; and then

1.8 mL of 2% 5-sulfosalicylic acid solution was added to the spiked samples. The mixture was ultrasonically extracted for 15 min and centrifuged at 12,000 rpm for 5 min. The supernatant was collected and filtered through a 0.22 μm membrane. The pH of the chicken extracts was adjusted to approximately 6 using 10 M NaOH solution. Ultimately, 180 μL of the samples were used for detection based on the same procedure as the ENR solution.

Statistical Analysis

Means ± standard deviations were calculated using Microsoft Excel 2010 (Microsoft Corp., Redmond, Wash.). Analysis of variance (ANOVA) was performed using SPSS Statistics 20 (SPSS, Chicago, Ill.). Significant differences were established at $p < 0.05$.

Results and Discussion

Characterization of BSA-ENR, QDs-BSA-ENR, and IMBs Complexes

ENR haptens were conjugated to BSA using an EDC and Sulfo-NHS-based amidation reaction, which was confirmed by the UV-vis spectrophotometry (Shen et al., 2019). As presented in figure 2a, ENR showed characteristic peaks at 271 nm, 322 nm, and 334 nm, and the distinguishing absorption peak of BSA was located at 278 nm. BSA-ENR complexes exhibited absorption peaks at 275 nm, 322 nm, and 334 nm. The shifted absorption peak of BSA-ENR complexes at 275 nm indicated that BSA-ENR complexes were successfully synthesized.

To ensure the conjugation of BSA-ENR and QDs, we adopted FTIR spectra and zeta potentials to characterize different modification processes, including QDs-COOH, EDC and Sulfo-NHS activated QDs (QDs-EDC/Sulfo-NHS), and QDs-BSA-ENR. FTIR spectra (fig. 2b) showed the characteristic peaks at 1704 and 1705 cm^{-1} for QDs-COOH and QDs-EDC/Sulfo-NHS, respectively, corresponding to the stretching vibration of C=O in carboxyl groups. After modification with BSA-ENR, the peak at 1651 cm^{-1} for QDs-BSA-ENR appeared as a result of the C=O stretching vibration in amide bonds. These amide bonds were from the BSA-ENR complex and formed between the amino groups in BSA-ENR and the carboxyl groups in QDs-COOH. The peak group at 1601 and 1493 cm^{-1} was attributed to the skeleton vibration of benzene rings originated from BSA-ENR, which indicated successful linkage of QDs and BSA-ENR. From figure 2c, the zeta potentials of QDs shifted from -37.6 to -27.4 mV with the step-by-step modifications, which were ascribed to the decrease of negatively charged COO^- groups on the QD surfaces. Both FTIR spectra and zeta potential measurements confirmed the successful conjugation between QDs and BSA-ENR.

The FTIR spectra and zeta potentials of MBs-COOH, EDC and Sulfo-NHS activated MBs (MBs-EDC/Sulfo-NHS), and IMBs were also measured to investigate the modification of magnetic beads. As shown in figure 2d, peaks at 1651 and 1539/1538 cm^{-1} for MBs-COOH and MBs-EDC/Sulfo-NHS, as well as at 1645 and 1516 cm^{-1} for IMBs, belonged to the amide I band and amide II band, respectively. MBs-COOH and MBs-EDC/Sulfo-NHS showed these characteristic peaks due to the pre-coated BSA on the MBs-

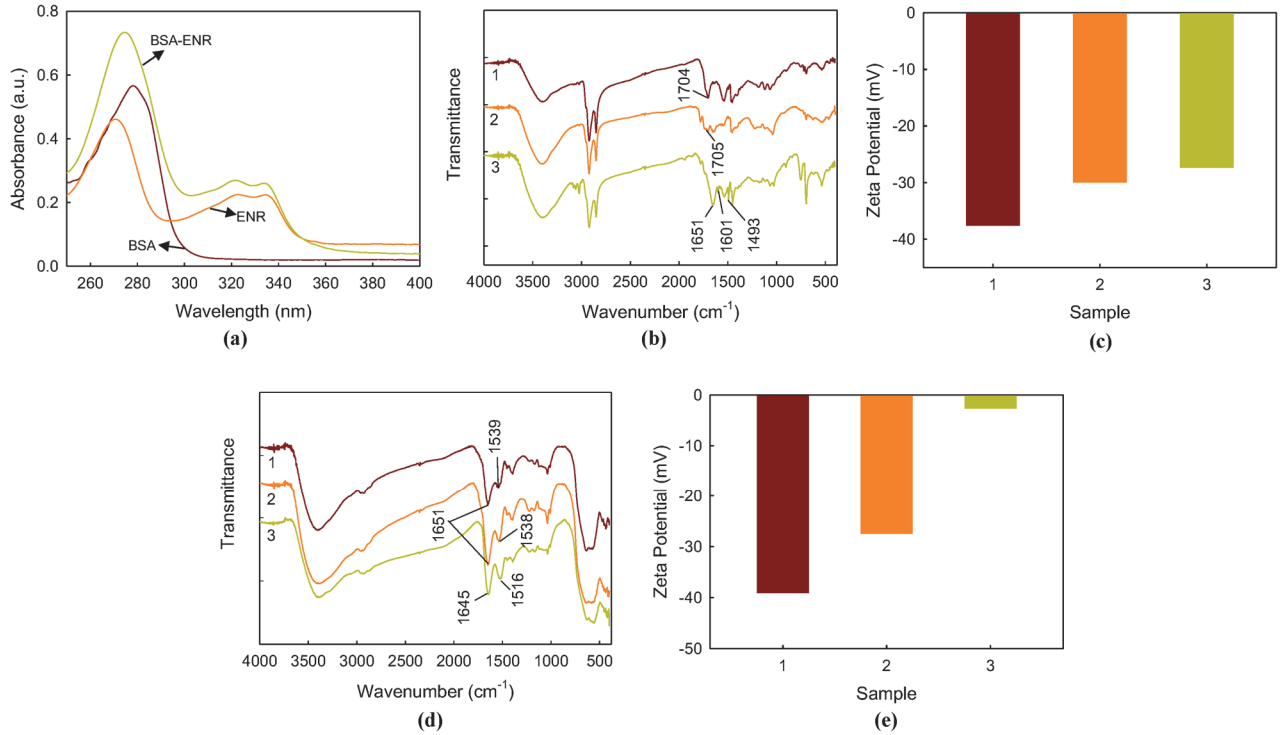

Figure 2. Characterization of BSA-ENR, QDs-BSA-ENR, and IMBs: (a) UV-vis spectra of BSA, ENR, and BSA-ENR; (b) FTIR spectra of (1) QDs-COOH, (2) QDs-EDC/Sulfo-NHS, and (3) QDs-BSA-ENR; (c) zeta potentials of (1) QDs-COOH, (2) QDs-EDC/Sulfo-NHS, and (3) QDs-BSA-ENR; (d) FTIR spectra of (1) MBs-COOH, (2) MBs-EDC/Sulfo-NHS, and (3) IMBs; and (e) zeta potentials of (1) MBs-COOH, (2) MBs-EDC/Sulfo-NHS, and (3) IMBs.

COOH surface according to the manufacturer's description, as BSA contains a number of peptide bonds. However, the relative height of the peak in the amide II region increased after modification, which was attributed to the newly formed amide bonds and the existing peptide bonds in antibodies, demonstrating that antibodies had been immobilized on the surfaces of the magnetic beads. The measurements of zeta potential further evidenced the step-by-step modifications of the magnetic beads (fig. 2e). The zeta potential of MBs-COOH was -39.1 mV due to the presence of COO^- groups on the surface. After activation, this value positively shifted to -27.5 mV, which was ascribed to the formation of amine-reactive esters. Further conjugation of antibodies to the magnetic beads led to a higher zeta potential of -2.67 mV as the antibodies might be positively charged under this condition. The above results confirmed that the conjugation of antibodies and magnetic beads succeeded.

Optimization of Assay Conditions

Because this nanobiosensor was based on the competitive binding of ENR and QDs-BSA-ENR complexes to IMBs, the concentrations of IMBs and QDs-BSA-ENR were two key factors that determined the final detection performance. Competitive inhibition rate and fluorescence intensity were chosen as the indicators to determine the optimum concentration of IMBs. The competitive inhibition rate was defined as $(F_0 - F)/F_0$, where F_0 and F represent the fluorescence intensities in the absence of ENR and with 25 ng mL^{-1} of target antigens, respectively. The most appropriate IMBs concentration should exhibit both higher competitive inhibition rate and fluorescence intensity. As shown in figure 3a, the concentration of IMBs was carefully optimized to be 0.1 mg mL^{-1}, at which acceptable competitive inhibition rate and fluorescence intensity were obtained. To explore the effect of QDs-BSA-ENR concentration on fluorescence signals, QDs-BSA-ENR probes with different volumes of 0.5, 1, 2, 4, 6, 8, and 10 µL were added to perform the immunoassay. With the increased volume of QDs-BSA-ENR probes, the fluorescence intensity increased and reached a plateau after 4 µL (fig. 3b). Hence, 4 µL of QDs-BSA-ENR probes served as the optimum in the subsequent experiments.

The activity of antibody molecules was significantly influenced by the changes in pH, further affecting the immunoreactions between the antigen and antibody. Thus, the effect of pH on fluorescence signals was also evaluated, as shown in figure 3c. The resultant fluorescence intensities under different pH conditions revealed that this immunoassay was most likely influenced at pH 3.0, as the fluorescence signals of both the negative control and with 25 ng mL^{-1} ENR almost disappeared. The biosensor worked at a pH range from 4.0 to 8.0. Given the highest fluorescence signal, pH 6.0 was eventually selected.

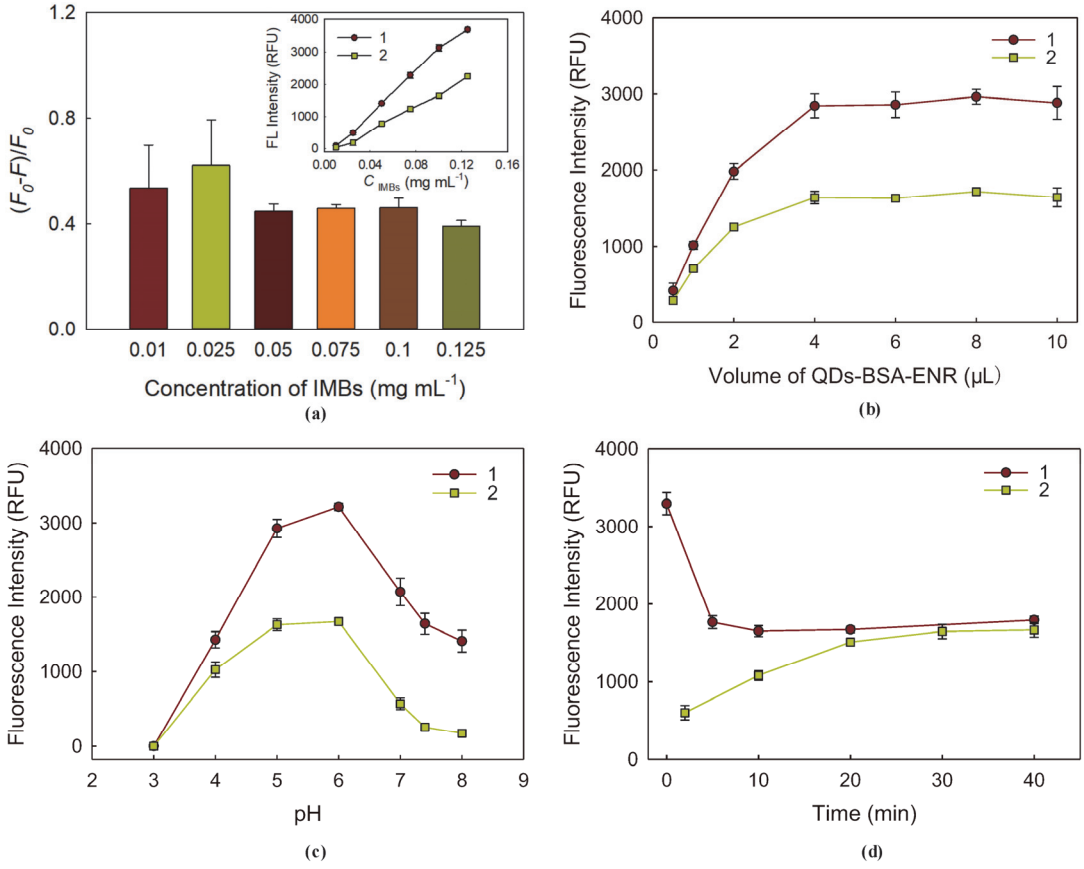

Figure 3. Optimization of the assay parameters: (a) effects of IMB concentration on the competitive inhibition rate and (inset) on the fluorescence intensity (1) in the absence of ENR and (2) with 25 ng mL^{-1} of target antigen; effects of (b) the volume of QDs-BSA-ENR and (c) pH on the fluorescence intensity (1) in the absence of ENR and (2) with 25 ng mL^{-1} of target antigen; and (d) optimization of (1) capture time for ENR and (2) reaction time for the binding of QDs-BSA-ENR to IMBs.

We finally optimized the capture time for ENR in samples and the reaction time between IMBs and QDs-BSA-ENR. As shown in figure 3d, ENR capture could be finished within 10 min due to the high reaction dynamics between IMBs and ENR in solution. However, the optimal reaction time for the binding of QDs-BSA-ENR to IMBs was 30 min, which might result from the larger steric hindrance between these two sensing elements.

Analytical Performance of Biosensing Method

Under the optimal conditions, a calibration curve showing the relationship between fluorescence responses and the logarithm of ENR concentrations (10^{-2} to 10^{5} ng mL^{-1}) was established. As shown in figure 4a, the fluorescence responses decreased as the concentration of ENR changed from 10^{-1} to 10^{5} ng mL^{-1}. The calibration curve was fitted using a four-parameter logistic model (Wang et al., 2018) (fig. 4b). As a result, the inset in figure 4b shows that the developed biosensing method exhibited a linear detection range from 1 to 100 ng mL^{-1}, and the regression equation was y = -0.316log$x$ + 0.984 (R^2 = 0.976), where y represents F/F_0 (F = fluorescence intensity at a concentration of ENR, and F_0 = fluorescence intensity in the absence of ENR), and x is the ENR concentration. The LOD was calculated to be 0.94 ng mL^{-1} (the concentration corresponding to three standard deviations below the mean of the blank control) (Lu et al., 2015), which was better than or comparable with several reported methods for the detection of ENR (table 1).

To further evaluate the specificity of this biosensor toward ENR, three fluoroquinolones (LEV, CIP, and NOR), as well as other kinds of antibiotics (OTC, TET, CAP, KAN, and DOX) were selected as interference reagents. The concentrations of both ENR and the interference antibiotics were 25 ng mL^{-1}. As shown in figure 5, compared with the blank control, NOR, CIP, and ENR showed significant differences ($p < 0.001$), while OTC, TET, and CAP were not significantly different ($p > 0.05$). It is clear that cross-

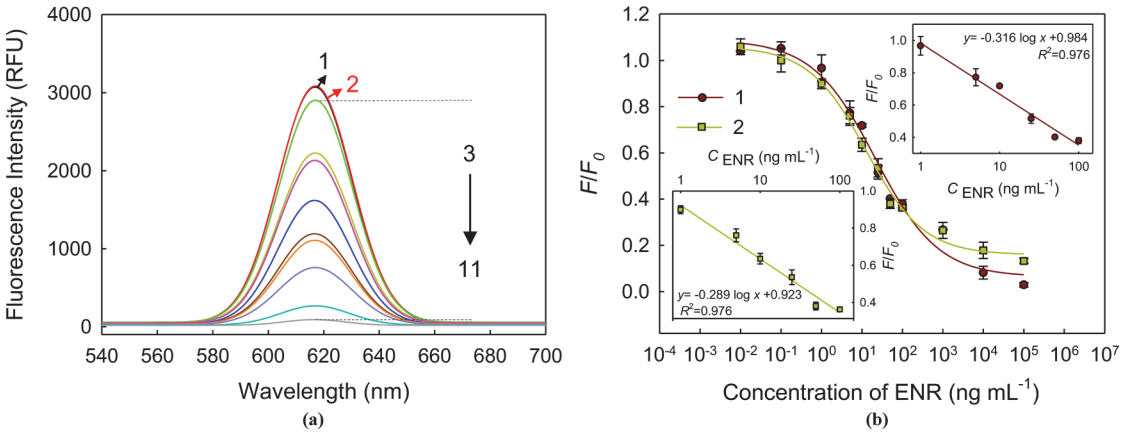

Figure 4. (a) Fluorescence responses of the biosensor to different concentrations of ENR in PBS buffer (ENR concentrations were 0.01, 0.1, 1, 5, 10, 25, 50, 10^2, 10^3, 10^4, and 10^5 ng mL^{-1} from 1 to 11, respectively) and (b) calibration plots for ENR detection in (1) PBS buffer and (2) chicken meat extracts, and (insets) the linear relationships between F/F_0 and the logarithm of ENR concentrations.

Table 1. Comparison of the performance of several methods for ENR detection.

Method	Linear Detection Range (ng mL^{-1})	Limit of Detection (ng mL^{-1})	Applications	Reference
Surface plasmon resonance immunosensor	-	1.2	Milk, chicken muscle, beef, pork, and fish	Pan et al., 2017
Upconversion fluorescence resonance energy transfer method	1 to 80	0.2	Water	Zhang et al., 2016
Direct competitive ELISA	2.5 to 40	0.7	Chicken muscle, egg, and cattle muscle	Kim et al., 2015
Aptamer chemiluminescent enzyme immunoassay	6.43 to 89.99	2.26	Bovine milk	Ni et al., 2014
Covalent organic framework-based electrochemical aptasensor	10^{-5} to 2	6.07×10^{-6}	Human serum	Wang et al., 2019
Upconversion nanoparticle-based aptasensor	1 to 10	0.06	Fish	Liu et al., 2016
Upconversion nanoparticle-based biosensor with double recognitions	0.5 to 10	0.04	Fish	Liu et al., 2017
Competitive chemiluminescence enzyme immunoassay	0.35 to 1	0.24	-	Yu et al., 2012
Fluoroimmunoassay	1 to 100	2.5	Chicken breast muscle	Chen et al., 2009
Electrochemical impedance spectroscopy	1 to 1000	1	Porcine serum	Wu et al., 2009
Immuno-strip biosensor system	100 to 10000	100	-	Kim and Kim, 2009
Lateral-flow colloidal gold immunoassay strip	0.038 to 22.75	0.935[a]	Chicken muscle	Zhao et al., 2008
Surface plasmon resonance immunosensor	-	1	Milk	Fernández et al., 2011
IMB-QDs biosensing method	1 to 100	0.94	Chicken meat	This study

[a] The color change observed by naked eye.

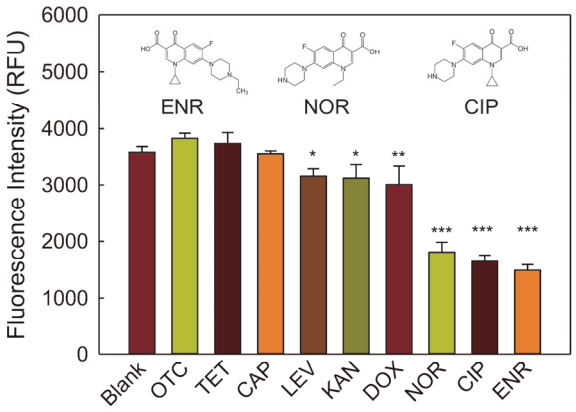

Figure 5. Fluorescence responses of biosensor to different antibiotics (OTC = oxytetracycline hydrochloride, TET = tetracycline hydrochloride, CAP = chloramphenicol, LEV = levofloxacin, KAN = kanamycin sulfate, DOX = doxycycline hydrochloride, NOR = norfloxacin, CIP = ciprofloxacin hydrochloride, and ENR = enrofloxacin). Asterisks indicate significance (* $p < 0.05$, ** $p < 0.01$, and *** $p < 0.001$) versus the blank control. Statistical analysis was performed using ANOVA followed by post hoc multiple comparison using Dunnett's test.

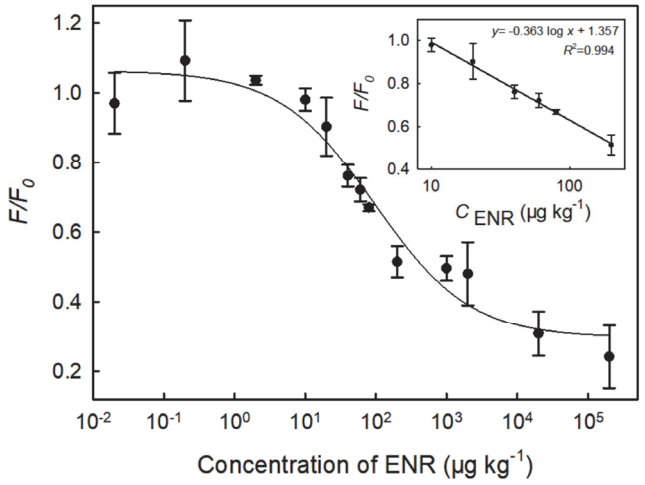

Figure 6. Plot of the calibration for detection of ENR in chicken meat and (inset) the linear relationship between F/F_0 and the logarithm of ENR concentration.

reaction of NOR and CIP existed, which might be a result of the similar structures of these two antibiotics with ENR. It is attributed to the specificity of the adopted antibody. The slight decreases in fluorescence response in the presence of LEV, KAN, and DOX might be caused by manual operation.

Detection Performance for ENR Residues in Chicken Meat

Our objective was to develop a rapid and sensitive method for detection of ENR in the poultry supply chain. Therefore, complex sample pretreatment procedures, such as solid phase extraction and organic solvent extraction, were not recommended. Considering the unique separation and concentration capabilities of IMBs, a simpler sample pretreatment method only using 5-sulfosalicylic acid as the extraction solvent was adopted. The 5-sulfosalicylic acid solution extracted ENR from chicken meat and removed proteins to reduce non-specific adsorption.

We first evaluated the interferences of the sample matrix after pretreatment on the immunoassay by detecting ENR spiked in chicken meat extracts at concentrations ranging from 10^{-2} to 10^{5} ng mL^{-1}. The calibration curve obtained in sample extracts was similar to that in PBS buffer (fig. 4b). The LOD was achieved at 1 ng mL^{-1} with a linear range from 1 to 100 ng mL^{-1}, which was comparable to those obtained in PBS buffer. These results indicated that the matrix effects could be fairly diminished.

To investigate the detection ability in actual food samples, ENR was also fortified in chicken meat and detected by the developed sensing method. A calibration curve was established, as shown in figure 6. The LOD was calculated to be 14.1 μg kg^{-1}, which was below the MRLs regulated in China and the European Union (100 μg kg^{-1}). The higher LOD obtained in the detection of ENR in chicken meat might have resulted from the insufficient extraction of ENR from the food samples, as well as the loss of antibiotics after pretreatment. However, for quantitation, this deficiency could be eliminated, as the standard curve was established based on the extracted ENR.

Table 2. Recovery assay of the nanobiosensor for ENR detection in chicken meat.[a]

ENR Added (μg kg^{-1})	ENR Detected (μg kg^{-1})	Recovery (%)	RSD[b] (%)
50	41.6 ±9.6	83.3	23.2
100	101.6 ±17.4	101.6	17.1
200	170.5 ±7.1	85.2	4.2

[a] The number of parallel tests for each group of experimental samples was 3 (n = 3).
[b] RSD = relative standard deviation.

To further evaluate the feasibility of the proposed nanobiosensor for ENR detection in actual samples, recoveries of ENR in spiked chicken meat samples were also determined. The results in table 2 show that the average recoveries of our proposed method ranged from 83.3% to 101.6%. Hence, the proposed method was applicable for ENR detection in actual raw chicken. Compared to the results from ELISA and liquid chromatography-tandem mass spectrometry (LC-MS/MS) methods, the efficiency of test for the biosensor method, as defined by Gopalakrishnan et al. (2002), was calculated to be 83% based on 66 chicken breast samples (data not shown). The material cost of each test was estimated to be $2.36 (table 3), which is less than or comparable with commercialized ELISA kits (table 4). However, the ELISA method requires more complicated sample pretreatment and detection procedures. As for LC-MS-based methods, although the material cost is less, expensive apparatus is required in an analytical laboratory. Therefore, the proposed biosensor method is cost-effective compared with ELISA and LC-MS-based methods.

Conclusions

In this study, a nanomaterial-based biosensing method was developed using IMBs and QDs-BSA-ENR as sensing elements for the detection of ENR in raw chicken. A 5-sulfosalicylic acid-based pretreatment method was used to

Table 3. Estimated cost of a single test for ENR detection.

Item	Name	Cost[a]	Consumption per Test	Cost per Test
Antibody	Mouse anti-enrofloxacin antibody	$2428 per mg	0.8 μg	$1.94
Magnetic beads	Carboxyl magnetic beads	$349 per 100 mg	20 μg	$0.07
Quantum dots	Carboxyl CdSe/ZnS Core/Shell QDs	$279 per 4 nmol	0.0008 nmol	$0.06
Other reagents and consumables (5-sulfosalicylic acid, BSA, low-binding tubes, ultrafiltration units, and other materials)				$0.29
			Total:	$2.36

[a] For mass production, this cost should be greatly reduced.

Table 4. Commercialized ELISA kits for ENR detection (based on information from the company websites).

Product	Size	Cost	Cost per Test	Company
Enrofloxacin ELISA kit (OKAO00116)	96 assays	$370	$3.85	Aviva Systems Biology Corp., San Diego, Cal.
ENR (Enrofloxacin) ELISA kit (E-FS-E032)	96 assays	$260	$2.71	Elabscience, Wuhan, China
Enrofloxacin (ENR) ELISA kit (E4277-100)	100 assays	$675	$6.75	BioVision, Inc., Milpitas, Cal.
Enrofloxacin (ER) ELISA kit (11253)	96 assays	$622	$6.48	Cepham Life Sciences, Inc., Fulton, Md.

reduce non-specific adsorption caused by complex food matrices. The designed sensor showed LODs of 0.94 ng mL^{-1} and 14.1 μg kg^{-1} in PBS buffer and chicken meat, respectively, which was below the MRLs of ENR regulated in China and the European Union. The total detection time for ENR in chicken samples was less than 1.5 h. Compared with conventional ELISA and chromatographic methods, this biosensing method showed advantages of rapidity, simplicity, sensitivity, and interference resistance. On-going research focuses on the development of a portable and automated biosensing instrument for in-field detection of ENR residues in the poultry supply chain to enhance food safety.

ACKNOWLEDGEMENTS

This research was funded by the Walmart Foundation (Project No. 0402-70013-21-0000) and supported by the Walmart Food Safety Collaboration Center. The authors thank Lisa Kelso for her review of the manuscript.

REFERENCES

Bonassa, K. P., Miragliotta, M. Y., Simas, R. C., Monteiro, D. A., Eberlin, M. N., Anadón, A., & Reyes, F. G. (2017). Tissue depletion study of enrofloxacin and its metabolite ciprofloxacin in broiler chickens after oral administration of a new veterinary pharmaceutical formulation containing enrofloxacin. *Food Chem. Toxicol., 105*, 8-13. https://doi.org/10.1016/j.fct.2017.03.033

Chen, J., Xu, F., Jiang, H., Hou, Y., Rao, Q., Guo, P., & Ding, S. (2009). A novel quantum dot-based fluoroimmunoassay method for detection of enrofloxacin residue in chicken muscle tissue. *Food Chem., 113*(4), 1197-1201. https://doi.org/10.1016/j.foodchem.2008.08.006

Chen, Z., Li, P., Zhang, Z., Zhai, X., Liang, J., Chen, Q., ... Wu, Y. (2019). Ultrasensitive sensor using quantum dots-doped polystyrene nanospheres for clinical diagnostics of low-volume serum samples. *Anal. Chem., 91*(9), 5777-5785. https://doi.org/10.1021/acs.analchem.9b00010

Cui, M., Lin, H., Wang, X., Cao, L., & Sui, J. (2015). 5-sulfosalicylic acid dihydrate-based pretreatment for the modification of enzyme-linked immunoassay of fluoroquinolones in fishery products. *J. Immunoass. Immunoch., 36*(5), 517-531. https://doi.org/10.1080/15321819.2015.1006330

Dolati, S., Ramezani, M., Nabavinia, M. S., Soheili, V., Abnous, K., & Taghdisi, S. M. (2018). Selection of specific aptamer against enrofloxacin and fabrication of graphene oxide based label-free fluorescent assay. *Anal. Biochem., 549*, 124-129. https://doi.org/10.1016/j.ab.2018.03.021

Ellerbrock, R. E., Canisso, I. F., Podico, G., Roady, P. J., Uhl, E., Lima, F. S., & Li, Z. (2019). Diffusion of fluoroquinolones into equine fetal fluids did not induce fetal lesions after enrofloxacin treatment in early gestation. *Vet. J., 253*, 105376. https://doi.org/10.1016/j.tvjl.2019.105376

Fernández, F., Pinacho, D. G., Sánchez-Baeza, F., & Marco, M. P. (2011). Portable surface plasmon resonance immunosensor for the detection of fluoroquinolone antibiotic residues in milk. *J. Agric. Food Chem., 59*(9), 5036-5043. https://doi.org/10.1021/jf1048035

Gopalakrishnan, V., Sekhar, W. Y., Soo, E. H., Vinsent, R. A., & Devi, S. (2002). Typhoid fever in Kuala Lumpur and a comparative evaluation of two commercial diagnostic kits for the detection of antibodies to *Salmonella* Typhi. *Singapore Med. J., 43*(7), 354-358.

Goryacheva, O. A., Novikova, A. S., Drozd, D. D., Pidenko, P. S., Ponomaryeva, T. S., Bakal, A. A., ... Goryacheva, I. Y. (2019). Water-dispersed luminescent quantum dots for miRNA detection. *Trends Anal. Chem., 111*, 197-205. https://doi.org/10.1016/j.trac.2018.12.022

Hu, S., Fang, B., Huang, Z., Chen, Y., Liu, D., Xing, K., ... Lai, W. (2019). Using molecular descriptors for assisted screening of heterologous competitive antigens to improve the sensitivity of ELISA for detection of enrofloxacin in raw milk. *J. Dairy Sci., 102*(7), 6037-6046. https://doi.org/10.3168/jds.2018-16048

Huang, W., Wang, P., Jiang, P., Dong, X., & Lin, S. (2018). Preparation and application of a restricted access material with hybrid poly(glycerol mono-methacrylate) and cross-linked bovine serum albumin as hydrophilic out layers for directly on-line high-performance liquid chromatography analysis of enrofloxacin and gatifloxacin in milk samples. *J. Chromatogr. A, 1573*, 59-65. https://doi.org/10.1016/j.chroma.2018.08.067

Huang, X., Aguilar, Z. P., Li, H., Lai, W., Wei, H., Xu, H., & Xiong, Y. (2013). Fluorescent $Ru(phen)_3^{2+}$-doped silica nanoparticles-based ICTS sensor for quantitative detection of enrofloxacin residues in chicken meat. *Anal. Chem., 85*(10), 5120-5128. https://doi.org/10.1021/ac400502v

Ji, T., Liu, D., Liu, F., Li, J., Ruan, Q., Song, Y., ... Wang, D. (2016). A pressure-based bioassay for the rapid, portable. and quantitative detection of C-reactive protein. *Chem. Commun., 52*(54), 8452-8454. https://doi.org/10.1039/c6cc03705d

Junza, A., Saurina, J., Barrón, D., & Minguillón, C. (2016). Metabolic profile modifications in milk after enrofloxacin administration studied by liquid chromatography coupled with high-resolution mass spectrometry. *J. Chromatogr. A, 1460*, 92-99. https://doi.org/10.1016/j.chroma.2016.07.016

Kim, C., & Searson, P. C. (2015). Magnetic bead-quantum dot assay for detection of a biomarker for traumatic brain injury. *Nanoscale, 7*(42), 17820-17826. https://doi.org/10.1039/c5nr05608j

Kim, N. G., Kim, M. A., Park, Y. I., Jung, T. S., Son, S. W., So, B., & Kang, H. G. (2015). Magnetic nanoparticle based purification and enzyme-linked immunosorbent assay using monoclonal antibody against enrofloxacin. *J. Vet. Sci., 16*(4), 431-437. https://doi.org/10.4142/jvs.2015.16.4.431

Kim, Y. K., & Kim, H. (2009). Immuno-strip biosensor system to detect enrofloxacin residues. *J. Ind. Eng. Chem., 15*(2), 229-232. https://doi.org/10.1016/j.jiec.2008.10.007

Li, N., Chow, A. M., Ganesh, H. V., Brown, I. R., & Kerman, K. (2013). Quantum dot based fluorometric detection of cancer TF-antigen. *Anal. Chem., 85*(20), 9699-9704. https://doi.org/10.1021/ac402082s

Li, S., Wang, Y., Mu, X., Sheng, W., Wang, J., & Wang, S. (2019). Two fluorescence quenching immunochromatographic assays based on carbon dots and quantum dots as donor probes for the determination of enrofloxacin. *Anal. Methods, 11*(18), 2378-2384. https://doi.org/10.1039/c9ay00154a

Lisi, F., Falcaro, P., Buso, D., Hill, A. J., Barr, J. A., Crameri, G., ... Mulvaney, P. (2012). Rapid detection of hendra virus using magnetic particles and quantum dots. *Adv. Healthc. Mater., 1*(5), 631-634. https://doi.org/10.1002/adhm.201200072

Liu, D., Huang, Y., Wang, S., Liu, K., Chen, M., Xiong, Y., ... Lai, W. (2015). A modified lateral flow immunoassay for the detection of trace aflatoxin M1 based on immunomagnetic nanobeads with different antibody concentrations. *Food Control, 51*, 218-224. https://doi.org/10.1016/j.foodcont.2014.11.036

Liu, X., Ren, J., Su, L., Gao, X., Tang, Y., Ma, T., ... Li, J. (2017). Novel hybrid probe based on double recognition of aptamer-molecularly imprinted polymer grafted on upconversion nanoparticles for enrofloxacin sensing. *Biosens. Bioelectron., 87*, 203-208. https://doi.org/10.1016/j.bios.2016.08.051

Liu, X., Su, L., Zhu, L., Gao, X., Wang, Y., Bai, F., ... Li, J. (2016). Hybrid material for enrofloxacin sensing based on aptamer-functionalized magnetic nanoparticle conjugated with upconversion nanoprobes. *Sens. Actuators B Chem., 233*, 394-401. https://doi.org/10.1016/j.snb.2016.04.096

Lu, C., Tang, Z., Liu, C., Kang, L., & Sun, F. (2015). Magnetic-nanobead-based competitive enzyme-linked aptamer assay for the analysis of oxytetracycline in food. *Anal. Bioanal.Chem., 407*(14), 4155-4163. https://doi.org/10.1007/s00216-015-8632-3

Moro, L., Turemis, M., Marini, B., Ippodrino, R., & Giardi, M. T. (2017). Better together: Strategies based on magnetic particles and quantum dots for improved biosensing. *Biotech. Adv., 35*(1), 51-63. https://doi.org/10.1016/j.biotechadv.2016.11.007

Ni, H., Zhang, S., Ding, X., Mi, T., Wang, Z., & Liu, M. (2014). Determination of enrofloxacin in bovine milk by a novel single-stranded DNA aptamer chemiluminescent enzyme immunoassay. *Anal. Lett., 47*(17), 2844-2856. https://doi.org/10.1080/00032719.2014.924009

Pan, M., Gu, Y., Zhang, M., Wang, J., Yun, Y., & Wang, S. (2018). Reproducible molecularly imprinted QCM sensor for accurate, stable, and sensitive detection of enrofloxacin residue in animal-derived foods. *Food Anal. Methods, 11*(2), 495-503. https://doi.org/10.1007/s12161-017-1020-1

Pan, M., Li, S., Wang, J., Sheng, W., & Wang, S. (2017). Development and validation of a reproducible and label-free surface plasmon resonance immunosensor for enrofloxacin detection in animal-derived foods. *Sensors, 17*(9), article 1984. https://doi.org/10.3390/s17091984

Paudel, S., Cerbu, C., Astete, C. E., Louie, S. M., Sabliov, C., & Rodrigues, D. F. (2019). Enrofloxacin-impregnated PLGA nanocarriers for efficient therapeutics and diminished generation of reactive oxygen species. *ACS Appl. Nano Mater., 2*(8), 5035-5043. https://doi.org/10.1021/acsanm.9b00970

Poller, A. M., Crooks, S., & Preininger, C. (2015). Influence of different surface chemistries on the ultrasensitive on-chip detection of enrofloxacin in milk. *Sens. Actuators B Chem., 209*, 1077-1083. https://doi.org/10.1016/j.snb.2014.10.101

Rezende, J. P., Pacheco, A. F. C., Magalhães, O. F., Coelho, Y. L., Vidigal, M. C. T. R., da Silva, L. H. M., & Pires, A. C. S. (2019). Polydiacetylene/triblock copolymer/surfactant nanoblend: A simple and rapid method for the colorimetric screening of enrofloxacin residue. *Food Chem., 280*, 1-7. https://doi.org/10.1016/j.foodchem.2018.12.033

Shen, X., Chen, J., Lv, S., Sun, X., Dzantiev, B. B., Eremin, S. A., ... Lei, H. (2019). Fluorescence polarization immunoassay for determination of enrofloxacin in pork liver and chicken. *Molecules, 24*(24), 4462. https://doi.org/10.3390/molecules24244462

Sultan, I. A. (2014). Detection of enrofloxacin residue in livers of livestock animals obtained from a slaughterhouse in Mosul City. *J. Vet. Sci. Tech., 5*(2), 168. https://doi.org/10.4172/2157-7579.1000168

Terrado-Campos, D., Tayeb-Cherif, K., Peris-Vicente, J., Carda-Broch, S., & Esteve-Romero, J. (2017). Determination of oxolinic acid, danofloxacin, ciprofloxacin, and enrofloxacin in porcine and bovine meat by micellar liquid chromatography with fluorescence detection. *Food Chem., 221*, 1277-1284. https://doi.org/10.1016/j.foodchem.2016.11.029

Wang, J., Sang, Y., Liu, W., Liang, N., & Wang, X. (2017). The development of a biomimetic enzyme-linked immunosorbent assay based on the molecular imprinting technique for the detection of enrofloxacin in animal-based food. *Anal. Methods, 9*(47), 6682-6688. https://doi.org/10.1039/c7ay02321a

Wang, M., Hu, M., Liu, J., Guo, C., Peng, D., Jia, Q., ... Du, M. (2019). Covalent organic framework-based electrochemical aptasensors for the ultrasensitive detection of antibiotics. *Biosens. Bioelectron., 132*, 8-16. https://doi.org/10.1016/j.bios.2019.02.040

Wang, X., Cohen, L., Wang, J., & Walt, D. R. (2018). Competitive immunoassays for the detection of small molecules using single molecule arrays. *J. American Chem. Soc., 140*(51), 18132-18139. https://doi.org/10.1021/jacs.8b11185

Wegner, K. D., & Hildebrandt, N. (2015). Quantum dots: Bright and versatile *in vitro* and *in vivo* fluorescence imaging biosensors. *Chem. Soc. Rev., 44*(14), 4792-4834. https://doi.org/10.1039/c4cs00532e

Wu, C. C., Lin, C. H., & Wang, W. S. (2009). Development of an enrofloxacin immunosensor based on label-free electrochemical impedance spectroscopy. *Talanta, 79*(1), 62-67. https://doi.org/10.1016/j.talanta.2009.03.006

Yang, K., Hu, Y., & Dong, N. (2016). A novel biosensor based on competitive SERS immunoassay and magnetic separation for accurate and sensitive detection of chloramphenicol. *Biosens. Bioelectron., 80*, 373-377. https://doi.org/10.1016/j.bios.2016.01.064

Yang, M., Liu, F., Wang, M., Zhou, J., Zhang, L., & Wang, T. (2020). Development of a whole liquid egg certified reference material for accurate measurement of enrofloxacin residue. *Food Chem., 309*, 125253. https://doi.org/10.1016/j.foodchem.2019.125253

Yasini, S. A., Zadeh, M. H. B., & Shahdadi, H. (2015). The antibacterial activity and toxicity of enrofloxacin are decreased by nanocellulose conjugated with aminobenzyl purin. *Colloids Surf. B, 135*, 518-524. https://doi.org/10.1016/j.colsurfb.2015.08.005

Yu, F., Wu, Y., Yu, S., Zhang, H., Zhang, H., Qu, L., & Harrington, P. D. B. (2012). A competitive chemiluminescence enzyme

immunoassay for rapid and sensitive determination of enrofloxacin. *Spectrochim. Acta A, 93*, 164-168. https://doi.org/10.1016/j.saa.2012.03.001

Yu, H. W., Jang, A., Kim, L. H., Kim, S. J., & Kim, I. S. (2011). Bead-based competitive fluorescence immunoassay for sensitive and rapid diagnosis of cyanotoxin risk in drinking water. *Environ. Sci. Tech., 45*(18), 7804-7811. https://doi.org/10.1021/es201333f

Zhang, Z., Zhang, M., Wu, X.-Y., Chang, Z., Lee, Y.-I., Huy, B. T., ... Jiang, G.-B. (2016). Upconversion fluorescence resonance energy transfer: A novel approach for sensitive detection of fluoroquinolones in water samples. *Microchem. J., 124*, 181-187. https://doi.org/10.1016/j.microc.2015.08.024

Zhao, Y., Zhang, G., Liu, Q., Teng, M., Yang, J., & Wang, J. (2008). Development of a lateral flow colloidal gold immunoassay strip for the rapid detection of enrofloxacin residues. *J. Agric. Food Chem., 56*(24), 12138-12142. https://doi.org/10.1021/jf802648z